Spatiotemporal Heterogeneity of Metro Station Area Vitality and Driving Mechanisms of Built Environment Using Multi-Source Data Fusion: A Case Study of Shanghai City

Zhiyue Ou, Zhongning Fu, Dongdong Tong, Xiangfei Yang, Yue Bai

Abstract—Accurately identifying the spatiotemporal driving mechanisms through which the built environment influences metro station area vitality is critical for advancing the coordinated development of urban human-land systems. Taking Shanghai—a representative megacity—as the case study, this research quantifies weekend station area vitality using Baidu heatmap data. A comprehensive built environment indicator system is constructed by integrating multi-source datasets, including points of interest (POIs), urban road networks, and streetscape imagery. To investigate the dynamic patterns and underlying drivers of vitality across spatial and temporal dimensions, this study employs a combination of **Exploratory Spatiotemporal Data Analysis** Optimal-Parameter Geographic Detector (OPGD), and Spatiotemporal Geographically Weighted Regression (GTWR). The results indicate that station area vitality demonstrates strong migratory inertia and spatial lock-in effects over time, with a high likelihood of maintaining its previous state. Key influencing factors include the density of functional facilities, distance to the city center, closeness centrality, sky openness, and floor area ratio. Moreover, interactions among built environment variables manifest in three primary forms: single-factor enhancement, nonlinear enhancement, and nonlinear suppression. The effects of these variables exhibit pronounced spatiotemporal heterogeneity, with most factors exerting both positive and negative impacts depending on the specific spatial-temporal context. These findings provide important insights for urban spatial governance and offer strategic guidance for enhancing station area vitality within a transit-oriented development (TOD) framework.

Index Terms—built environment; metro station area vitality; multi-source data; spatiotemporal driving

Manuscript received May 23, 2025; revised August 7, 2025.

This research was supported by the Major Special Projects of Science and Technology in Gansu Province (No. 25ZDFA010), and the National Natural Science Foundation Regional Science Foundation Project (No. 71961016).

Zhiyue Ou is a postgraduate student at the School of Traffic and Transportation, Lanzhou Jiaotong University, Lanzhou 730070, China. (e-mail: ozy20230312@163.com).

Zhongning Fu is an associate professor at the School of Traffic and Transportation, Lanzhou Jiaotong University, Lanzhou 730070, China. (Corresponding author, phone: +86 13669379442, e-mail: fuzhongning@163.com).

Dongdong Tong is a postgraduate student at the School of Traffic and Transportation, Lanzhou Jiaotong University, Lanzhou 730070, China. (e-mail: 3514966755@qq.com).

Xiangfei Yang is an associate professor at the School of Traffic and Transportation, Lanzhou Jiaotong University, Lanzhou 730070, China. (e-mail: yangxfei06@163.com).

Yue Bai is a postgraduate student at the School of Traffic and Transportation, Lanzhou Jiaotong University, Lanzhou 730070, China. (e-mail: 2413475237@qq.com).

I. INTRODUCTION

In the context of rapid urbanization, the metro, as the core of modern urban transportation systems, is not only a vital component of the urban spatial structure but also a key link connecting various urban spaces. It accommodates a large share of residents' daily travel needs and supports diverse urban activities [1]. With the continued expansion of China's rail transit network, metro station areas are increasingly exhibiting multifunctional and mixed-use spatial characteristics [2]. The areas surrounding stations have evolved beyond mere transportation hubs into urban "micro-centers" that integrate commerce, services, social interaction, and cultural activities [3].

The concept of "metro station area vitality" refers to the comprehensive and dynamic manifestation of vitality that emerges within a certain spatial range around a metro station, driven by the interaction and coupling between the station itself and nearby urban functional units [4]. Compared to the traditional notion of "urban vitality," metro station area vitality places greater emphasis on transport dependency, spatial accessibility, and high-frequency dynamism [5][6]. In terms of representation, early studies primarily relied on traditional methods such as field observations [7], questionnaire surveys [8], and face-to-face interviews [9]. While these approaches can partially reveal vitality characteristics at a local scale, their effectiveness is constrained by limited sample sizes, data accuracy, and the subjectivity of respondents, making it difficult to capture the overall patterns and intrinsic features of urban vitality. In recent years, with the rise of big data and the rapid 3S multi-source advancement technologies, spatiotemporal data—such as mobile signaling data [10], social media data [11], and population heatmaps [12]—have been widely applied in urban vitality research. These emerging data sources offer advantages such as high timeliness, broad coverage, and strong objectivity, significantly enriching the dimensions and scope of vitality measurement and providing new perspectives and tools for the fine-grained assessment of metro station area vitality.

Meanwhile, existing studies on urban vitality and metro ridership have provided strong theoretical and methodological support for the construction and analysis of metro station area vitality. Current research primarily focuses on two directions: one is the quantification and construction of built environment indicator systems, and the other is the exploration of how the built environment

influences travel behavior. Early studies established the "3D" built environment evaluation framework—centering on density, diversity, and design—which laid the theoretical foundation for understanding the relationship between urban spatial structure and transport vitality [13]. Building upon this, scholars later introduced two additional dimensions: destination accessibility and distance to transit, thereby developing a more comprehensive "5D" built environment indicator system, which has become the mainstream paradigm in current urban transport research [14].

In terms of methodology, traditional studies often adopt classical statistical approaches such as Ordinary Least Squares (OLS) regression [15] and spatial autoregression [16], which mainly aim to reveal the overall linear relationship between the built environment and travel behavior. However, as understanding of the complexity of urban systems deepens, researchers have increasingly recognized the nonlinear nature of this relationship. In response, some studies have begun incorporating machine learning models to uncover potential nonlinear relationships between the built environment and travel behavior from a more flexible modeling perspective [17][18]. Although these models offer significant advantages in terms of improving fitting accuracy and predictive power, they remain essentially global models and thus struggle to address the non-stationarity and local heterogeneity commonly present in urban spatial structures [19]. To overcome these limitations, some scholars have turned to local spatial models such as Geographically Weighted Regression (GWR) [20] and Multiscale Geographically Weighted Regression (MGWR) [21], which introduce spatial weighting functions to capture spatially varying relationships between variables across different geographic locations. These methods are more aligned with the complex realities of urban dynamics.

In summary, although existing research on urban vibrancy has generated numerous valuable insights, notable gaps remain in the following three areas: (1) Systematic investigations specifically addressing vibrancy in metro station areas are still relatively scarce. Most studies either adopt a broad perspective on "urban vibrancy" or focus narrowly on "metro ridership," offering limited in-depth analysis at the station-area scale. (2) Many studies examine built environment factors in isolation, overlooking the synergistic effects that emerge from the interaction among multiple variables. (3) The prevailing spatial and temporal analytical approaches are often static and conventional, resulting in a disconnection between spatial and temporal dimensions—a phenomenon that can be described as "spatiotemporal fragmentation."

To address these research gaps, this study selects Shanghai—a representative Transit-Oriented Development (TOD) city—as the case study. Adopting a spatiotemporal interaction perspective, Exploratory Spatiotemporal Data Analysis (ESTDA) is employed to investigate the dynamic patterns of vibrancy in metro station areas. Building upon this, the study integrates the Optimal Parameter-based Geographical Detector (OPGD) and the Geographically and Temporally Weighted Regression (GTWR) model to uncover the spatiotemporal driving mechanisms of built environment factors influencing metro station area vibrancy at both global and local scales. The findings aim to provide a scientific foundation for refined spatial governance and the sustainable enhancement of station-area vibrancy in metro-oriented cities.

II. DATA AND METHOD

A. Study Area and Research Scope

Shanghai is located at the estuary of the Yangtze River and serves as a strategic intersection between the Yangtze River Economic Belt and the Coastal Economic Axis (Figure 1). As of December 2024, the Shanghai Metro system comprises 21 lines, with a total of 517 stations and an operating length of 896 kilometers. In this study, an 800 meter buffer around each metro station is used as the spatial analysis unit. This delineation is based on the widely accepted threshold of walking accessibility (10-15 minutes) and the service radius of rail transit under the Transit-Oriented Development framework [22]. To address the issue of spatial overlap among multiple station service areas, Thiessen polygon partitioning is applied to eliminate spatial coupling effects between adjacent stations.

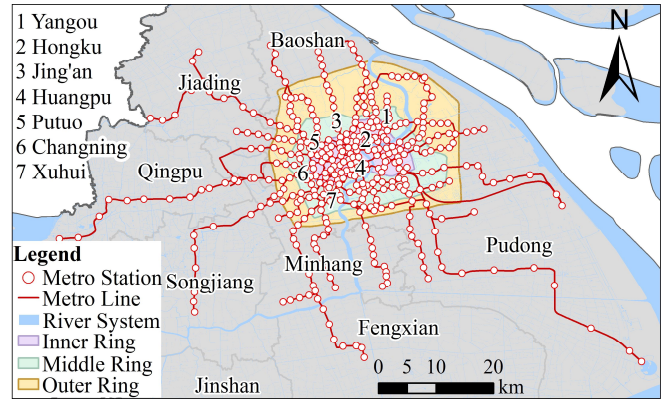


Fig. 1. The study area

B. Data Sources and Indicator System Construction

B.1. Quantification of Metro Station Area Vitality

Population heatmap data from the Baidu Huiyan platform (https://huiyan.baidu.com/products/platform) is used as the quantitative benchmark for measuring metro station area vitality. This dataset is derived from the spatiotemporal aggregation of anonymized mobile phone location and location service requests, and dynamic heatmaps are generated through kernel density analysis to objectively reflect the intensity of human activity. Considering that weekday foot traffic is heavily influenced by institutional activities such as commuting-making it difficult to accurately capture the impact of the built environment on spontaneous and recreational activities [23]—four weekends between April and July 2024 (April 13-14, May 18-19, June 15–16, and July 27–28) are selected as the study period. Based on the first and last train schedules of the Shanghai Metro, data is sampled hourly from 6:00 to 23:00 each day. To ensure the ecological validity of the data, a dual control strategy is employed: (1) dates are selected to avoid periods extreme weather, severe air pollution, and the commencement of new metro lines; (2) sampling is conducted across multiple months to minimize short-term event-driven disturbances and to emphasize the stable mechanisms through which spatial structure affects vitality.

Based on relevant literature [24], the original data were processed through the following steps: (1) hourly population heatmap CSV files were imported into ArcGIS and converted into point features; (2) kernel density analysis was conducted on these point features to produce a continuous surface representing spatial density; (3) the resulting kernel density surface was spatially joined with metro station areas

to perform zonal statistics, thereby obtaining the spatial distribution of vibrancy. Finally, the average vibrancy across four consecutive weekends was calculated to represent the vibrancy intensity of each metro station area.

B.2. Quantification of Built Environment Metrics

Building on previous studies [12][25][26], this study develops an indicator system grounded in the "5D" framework of the built environment. It encompasses five dimensions: land use intensity, population and facility distribution, transportation and accessibility, street environment quality, and metro station characteristics. A total of 22 indicators are selected, as presented in Table I.

Building outline and road network data were obtained from OpenStreetMap; POI data were collected through Amap (https://lbs.amap.com/) and cleaned to retain about 1.71 million valid entries. Population raster data were sourced from WorldPop and calibrated using zonal statistics in combination with district-level population census data from the Shanghai Municipal Statistics Bureau as of early 2024. Street view images were acquired through the Baidu Panorama platform (https://quanjing.baidu.com/). Metro network data were retrieved from the official website of Shanghai Metro (http://www.shmetro.com/). All data used in this study were collected in 2024. To ensure the robustness and reliability of the subsequent modeling process, multicollinearity among the independent variables was assessed using the Variance Inflation Factor (VIF). Two variables-street closeness and interface enclosure-were excluded due to their high VIF values, indicating potential multicollinearity issues. For the remaining 20 indicators, VIF values ranged from 1.3 to 5.2, suggesting that multicollinearity was within an acceptable and manageable range. The detailed calculation methods for the selected indicators are described as follows:

(1) Functional Mix Index

The functional mix index is a key metric used to evaluate the balance and diversity of facility types within a given area, reflecting the degree of land-use heterogeneity and urban vitality. Drawing on the Gaode POI (Point of Interest) Classification and Coding system, facilities are categorized into 23 primary classes and 261 secondary subcategories, including catering services, commercial enterprises, and daily life services. The functional mix within each spatial analysis unit is quantified using location entropy, which captures the distributional evenness of different facility types. A higher entropy value indicates a more balanced and diverse functional composition. The calculation formula is as follows:

$$E_{i} = -\frac{1}{\ln(N)} \sum_{j=1}^{N} p_{ij} \ln p_{ij}$$
 (1)

Where: E_i represents the functional mix degree of metro station area i; N denotes the total number of POI categories; p_{ij} indicates the proportion of POIs of category j within metro station area i to the total number of POIs in that area.

(2) Street Network Morphology

The Spatial Design Network Analysis (sDNA) method was utilized to quantify two key indicators of Shanghai's street network—closeness and betweenness—in order to capture the morphological characteristics of the actual urban road system [27]. Street closeness reflects the topological integration of a street node by evaluating its minimum cumulative topological depth relative to all other nodes

within the network. This indicator serves as a proxy for spatial accessibility, highlighting how easily a location can be reached from elsewhere in the network. The corresponding formula is as follows:

$$NQPDA(x) = \sum_{y \in R_x} \frac{W(y)p(y)}{d_m(x, y)}$$
 (2)

Where: NQPDA(x) represents the closeness value of node x; R_x denotes the set of all nodes within the search radius R centered on node x; W(y) is the weight of the road segment associated with node y; p(y) is the weight of node y; $d_m(x,y)$ indicates the shortest topological distance from node x to node y.

Street betweenness is quantified using the topological choice metric, which captures the likelihood of a street segment being traversed as part of the shortest paths between all pairs of nodes in the network. This measure reflects the street's potential to function as an intermediary or transfer point within the broader circulation system, indicating its importance as a traffic distribution hub. A higher betweenness value suggests a greater capacity to facilitate movement and connect different parts of the urban fabric. The calculation formula is as follows:

$$TPB_{t}(x) = \sum_{y \in N} \sum_{z \in R_{y}} OD(y, z, x) \frac{W(z)P(z)}{TotalWeight(y)}$$
(3)

Where: $TPB_t(x)$ represents the through-movement value of node x; N denotes the set of all nodes in the network; R_y refers to the set of nodes connected to node y; OD(y,z,x) indicates the shortest path between y and z that passes through x within the search radius; TotalWeight(y) is the total node weight within the search radius of node y.

(3) Street Environment Quality

Based on the road centerline data of Shanghai, street view sampling points were generated at 100 meter intervals. A Python script was developed to capture street view images in four directions (0°, 90°, 180°, and 270°), resulting in a total of 98,676 images. These images were horizontally stitched into panoramic views with a resolution of 2048 × 512 pixels. To enhance the understanding and segmentation accuracy of complex urban scenes, a PSPNet model was constructed, integrating a multi-scale dilated convolution module with an encoder-decoder architecture [28]. The model was pre-trained using transfer learning on the ADE20K dataset to facilitate multi-scale perception and hierarchical semantic interpretation of street view elements. Based on the extracted semantic information from the street view imagery, visual entropy was subsequently calculated to quantify the complexity and structural disorder of the street environment. The corresponding calculation formula is as follows:

$$SVE_{i} = -\frac{1}{\ln K} \sum_{k=1}^{K} \left(\frac{p_{i,k}}{P_{i} - p_{i,sky}} \ln \frac{p_{i,k}}{P_{i} - p_{i,sky}} \right)$$
(4)

Where: SVE_i represents the normalized visual information entropy of streetscape point i; K denotes the total number of visual element categories; P_i is the total number of original pixels at streetscape point i; $P_{i,sky}$ indicates the number of sky pixels at streetscape point i; $P_{i,k}$ represents the number of pixels belonging to the k-th visual element at streetscape point i.

(4) Metro Station Network Centrality

In the analysis of metro network centrality, closeness centrality and betweenness centrality are two widely adopted indicators used to evaluate the structural importance of individual stations within the network topology. These measures offer insights into the accessibility and mediating roles of stations in facilitating passenger flow across the system. Their respective formulations are presented as follows:

$$C_C(i) = \frac{n-1}{\sum_{i \neq i} d(i,j)}$$
 (5)

Where: $C_c(i)$ is the closeness centrality of subway station i; n is the total number of subway stations in the network; d(i,j) is the shortest path distance between subway stations i and j.

$$C_B(i) = \sum_{s \neq i \neq t} \frac{\sigma_{st}(i)}{\sigma_{st}}$$
 (6)

Where: $C_B(i)$ is the betweenness centrality of subway station i; s, t are two distinct subway stations in the network; σ_{st} is the total number of shortest paths between subway stations *s* and *t* that pass through station *i*.

C. Research Methods and Models

C.1. Exploratory Spatiotemporal Data Analysis

The ESTDA extends traditional static spatial analysis by incorporating the temporal dimension, enabling the integrated and dynamic examination of spatial and temporal elements [29]. The methodological framework encompasses techniques such as spatial autocorrelation (Moran's I), LISA time paths and spatiotemporal transitions, and spatial Markov chains. These approaches are capable of revealing the temporal evolution of spatial units and the dynamic transformation of spatial structures over time.

The LISA time path traces the movement of local spatial units within the Moran's I scatter plot, thereby illustrating the joint temporal variation of station-area vitality and its spatial lag term. This approach provides a continuous dynamic representation of the LISA Markov transition matrix. The geometric properties of the LISA time path are primarily characterized by two indicators: relative length and curvature, which are calculated as follows:

$$N_{i} = \frac{n \times \sum_{t=1}^{T-1} d(L_{i,t}, L_{i,t+1})}{\sum_{i=1}^{n} \sum_{t=1}^{T-1} d(L_{i,t}, L_{i,t+1})}$$

$$D_{i} = \frac{\sum_{t=1}^{T-1} d(L_{i,t}, L_{i,t+1})}{d(L_{i,t}, L_{i,T})}$$
(8)

$$D_{i} = \frac{\sum_{t=1}^{T-1} d(L_{i,t}, L_{i,t+1})}{d(L_{i,1}, L_{i,T})}$$
(8)

Where: N_i and D_i represent the relative length and curvature, respectively; n denotes the number of metro station areas; T is the time interval; $L_{i,t}$ represents the LISA coordinate $(y_{i,t},yL_{i,t})$ of metro station area i at time t; $d(L_{i,t},L_{i,t+1})$ indicates the movement distance of metro station area *i* from time *t* to t+1.

LISA spatiotemporal transitions are used to capture the dynamic evolution of local spatial relationships among neighboring units. These transitions can be classified into four main types, as summarized in Table II.

TABLE I SELECTION AND DESCRIPTION OF BUILT ENVIRONMENT INDICATORS

Dimension	ension Indicator Name Indicator Description				
Land use intensity	Floor area ratio	(Building footprint area×number of floors) within the buffer zone divided by the station area.			
	Functional mix	The richness/diversity of POI facilities within the buffer zone.			
Population and facility distribution	Resident population density	Total population within the buffer zone divided by the station area (10,000 people/km²).			
	Commercial service facility density	Number of shopping, dining, and similar facilities within the buffer zone per unit area (facilities/km²).			
	Business and office facility density	Number of companies, financial institutions, etc., within the buffer zone per unit area (facilities/km 2).			
	Educational and cultural facility density	Number of schools, research institutions, etc., within the buffer zone per unit area (facilities/ km^2).			
	Leisure and entertainment facility density	Number of sports, leisure, parks, and scenic spots within the buffer zone per unit area (facilities/km²).			
	Bus stop density	Number of bus stops within the buffer zone divided by the station area (stops/km²).			
	Road density	Total length of roads within the buffer zone divided by the station area (km/km²).			
Transportation	Street closeness	Average kernel density estimation value of NQPDE800 within the buffer zone, calculated using sDNA.			
and accessibility	Street betweenness	Average kernel density estimation value of TPBtE800 within the buffer zone, calculated using sDNA.			
	Distance to city center	Straight-line distance from the station to People's Square (km).			
	Distance to tertiary hospital	Straight-line distance from the station to the nearest tertiary hospital (km).			
	Green view index	Average proportion of pixels occupied by grass, vegetation, and trees in street view points within the buffer zone.			
Street	Street safety index	Average proportion of pixels occupied by safety-related elements such as traffic signs, streetlights, surveillance cameras, and guardrails in street view points within the buffer zone.			
environmental	Sky openness	Average proportion of pixels occupied by the sky in street view points within the buffer zone.			
quality	Interface enclosure	Average proportion of pixels occupied by elements such as walls, buildings, and columns in street view points within the buffer zone.			
	Street visual entropy	Visual complexity and diversity of the environment at street view points within the buffer zone.			
Metro station	Closeness centrality	Closeness centrality of the station, reflecting the ease of reaching other stations.			
	Betweenness centrality	Betweenness centrality of the station, indicating its role as a "bridge" within the metro network.			
characteristics	Metro station age	Number of years since the station was opened (years).			
	Number of entrances/exits	Total number of station entrances and exits (units).			

C.2. Optimal Parameter-based Geographical Detector

The Geographical Detector is a statistical tool designed to uncover spatial heterogeneity and identify its underlying driving factors. However, traditional implementations of the method often rely on subjective judgment when discretizing continuous variables, potentially compromising the reliability of the results. To overcome this limitation, the Optimal Parameter-based Geographical Detector (OPGD) is adopted, which enables adaptive discretization of continuous variables [30].

This approach, integrating the dual modules of Factor Detection and Interaction Detection, is employed to examine how built environment elements affect station-area vibrancy. The Factor Detection module evaluates the explanatory power of individual built environment factors on the spatial variation in station-area vibrancy, using the q-statistic to quantify each factor's independent contribution. A higher q value indicates a stronger explanatory influence. The calculation formula is as follows:

$$q = 1 - \frac{\sum_{h=1}^{L} N_h \sigma_{V,h}^2}{N \sigma_V^2} = 1 - \frac{SSW}{SST}$$
 (9)

Where: V represents the intensity of metro station area vibrancy; L denotes the optimal number of strata; σ_v^2 is the total variance of vibrancy; $\sigma_{v,h}^2$ is the within-stratum variance; N_h refers to the number of samples within a stratum; SSW and SST represent the sum of within-stratum variances and the total sum of variances, respectively.

The Interaction Detection module is employed to evaluate how the combined effect of two built environment factors alters their explanatory power with respect to station-area vibrancy. By comparing the joint q-statistic of the two factors with their individual q-statistics, this analysis identifies the nature of their interaction—whether it is synergistic (enhancing each other's influence), independent (non-interactive), or antagonistic (diminishing each other's effect). Such distinctions are crucial for understanding the complexity of spatial processes, as interactions often exhibit non-linear and context-dependent characteristics. The specific criteria used to classify interaction types are presented in Table III.

C.3. Spatiotemporal Geographically Weighted Regression Model

Geographically and Temporally Weighted Regression (GTWR) extends the traditional Geographically Weighted Regression (GWR) by simultaneously accounting for spatial and temporal heterogeneity in regression relationships [31].

Unlike GWR, which applies local weighting solely based on geographic location, GTWR integrates both spatial and temporal information in the construction of local regression parameters. This enables a more effective examination of the non-stationary relationships between independent and dependent variables across space and time. During model estimation, bandwidth parameters are typically selected using the corrected Akaike Information Criterion (AICc) or cross-validation. The basic formulation of the GTWR model is as follows:

$$y_{i} = \beta_{0}(u_{i}, v_{i}, t_{i}) + \sum_{k=1}^{p} \beta_{k}(u_{i}, v_{i}, t_{i}) x_{ik} + \varepsilon_{i}$$
 (10)

Where: y_i is the dependent variable at location (u_i, v_i) and time t_i ; $\beta_0(u_i, v_i, t)$ is the intercept term varying over space and time; $\beta_k(u_i, v_i, t)$ is the local regression coefficient for the k-th independent variable at (u_i, v_i, t_i) ; x_{ik} is the value of the k-th independent variable at observation i; ε_i is the random error term

$$\hat{\boldsymbol{\beta}}(u_i, v_i, t_i) = \left(\mathbf{X}^{\top} \mathbf{W}(u_i, v_i, t_i) \mathbf{X}\right)^{-1} \mathbf{X}^{\top} \mathbf{W}(u_i, v_i, t_i) \mathbf{y} \quad (11)$$

Where: $\hat{\boldsymbol{\beta}}(u_i, v_i, t_i)$ is the vector of estimated local regression coefficients at (u_i, v_i, t_i) ; **X** is the matrix of independent variables for all observations; **y** is the vector of dependent variables for all observations; $\mathbf{W}(u_i, v_i, t_i)$ is the diagonal spatial-temporal weight matrix for observation i, constructed by kernel functions.

$$w_{ij} = \exp\left(-\frac{d_{ij}^2}{h^2}\right) \tag{12}$$

Where: w_{ij} is the spatiotemporal weight between observation i and j; d_{ij} is the spatiotemporal distance between observations i and j; h is the bandwidth parameter controlling the kernel smoothing.

$$d_{ij} = \sqrt{(x_i - x_j)^2 + (y_i - y_j)^2 + \lambda (t_i - t_j)^2}$$
 (13)

Where: (x_i,y_i) and (x_j,y_j) are spatial coordinates of observations i and j; t_i and t_j are temporal coordinates of observations i and j; λ is a scaling parameter that balances spatial and temporal distances.

TABLE II
SPATIOTEMPORAL TRANSITION TYPES OF LISA

STATIOTEWITORAL TRANSPITION TITES OF LISA					
Type	Symbolic Expression	Transition Form			
TYPE I	$HH_t \rightarrow LH_{t+1}$, $LH_t \rightarrow HH_{t+1}$, $HL_t \rightarrow LL_{t+1}$, $LL_t \rightarrow HL_{t+1}$	Self-transition with unchanged neighborhood			
TYPE II	$HH_t \rightarrow HL_{t+1}$, $LH_t \rightarrow LL_{t+1}$, $HL_t \rightarrow HH_{t+1}$, $LL_t \rightarrow LH_{t+1}$	Neighborhood transition with unchanged self			
TYPE III	$HH_t \rightarrow LL_{t+1}, LL_t \rightarrow HH_{t+1}, LH_t \rightarrow HL_{t+1}, HL_t \rightarrow LH_{t+1}$	Simultaneous transition of self and neighborhood			
TYPE IV	$HH_t \rightarrow HH_{t+1}, HL_t \rightarrow HL_{t+1}, LL_t \rightarrow LL_{t+1}, LH_t \rightarrow LH_{t+1}$	No transition in either self or neighborhood			

TABLE III
GEODETECTOR INTERACTION TYPES

Criteria for Determination	Interaction Type		
$q(X_1 \cap X_2) < \min[q(X_1), q(X_2)]$	Nonlinear weakening		
$\min[q(X_1), q(X_2)] < q(X_1 \cap X_2) < \max[q(X_1), q(X_2)]$	Single-factor nonlinear weakening		
$q(X_1 \cap X_2) > \max[q(X_1), q(X_2)]$	Two-factor enhancement		
$q(X_1 \cap X_2) = q(X_1) + q(X_2)$	Independence		
$q(X_1 \cap X_2) > q(X_1) + q(X_2)$	Nonlinear enhancement		

III. RESULTS

A. Spatiotemporal Interaction Characteristics of Metro Station Area Vitality

A.1. Spatiotemporal Static Characteristics

The vibrancy of metro station areas in Shanghai exhibits clear temporal differentiation in terms of spatiotemporal autocorrelation patterns (Figure 2). At all time periods, the Global Moran's I values are significantly positive at the 1%level, indicating a notable spatial clustering of station-area vibrancy. Specifically, during 6:00–9:00, as urban activities begin to awaken, vibrancy levels surge from 107.2 to 297.5, accompanied by an increase in spatial clustering (Moran's I rises from 0.437 to 0.502). Between 10:00-17:00, vibrancy continues to grow slowly, reaching a peak of 378.3; however, the degree of spatial clustering decreases (Moran's I drops to 0.415). At night, overall vibrancy declines, yet after 21:00, Moran's I shows a clear rebound—from 0.366 to 0.436—indicating a renewed intensification of spatial clustering. Overall, the temporal variation in metro station-area vibrancy in Shanghai follows a pattern of "rise-stability-decline," while the spatial clustering demonstrates a trend of "enhance-weaken-re-enhance."

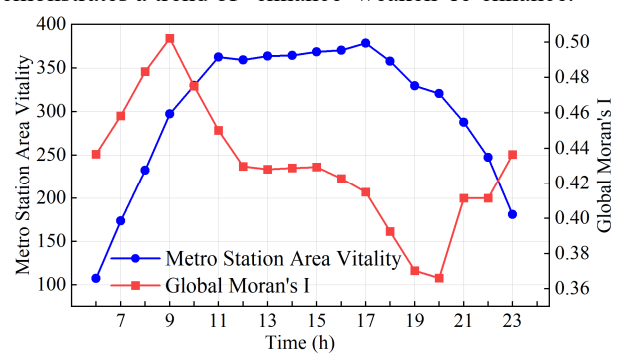


Fig. 2. Time series variation of subway station area vitality and global moran's index

Referring to existing research, the study period is preliminarily divided into four time segments for visualization: morning (6:00–12:00), afternoon (13:00–18:00), evening (19:00–23:00), and the entire day. Based on the distribution characteristics of vitality values across these time periods, metro station area vitality is categorized into five levels: low vitality (0–200.00), lower-middle vitality (200.01–400.00), medium vitality (400.01–600.00), upper-middle vitality (600.01–1000.00), and high vitality (1000.01–2400.00).

As shown in Figure 3, the spatial distribution of metro station area vitality in Shanghai exhibits a compound pattern characterized by a "core radiation + axial extension" structure. High-vitality station areas form a multi-level spatial system centered around People's Square-East Nanjing Road, with major nodes such as Xujiahui, Jing'an Temple, and large transportation hubs. These areas extend along metro lines 1, 2, 9, and 10 to form continuous vitality corridors. Temporally, there are only 18 high and medium-high vitality station areas in the morning, accounting for 4.44%, mainly concentrated in the city center. As urban activity intensifies, the number rises to 57 in the afternoon (14.07%), indicating a significant spatial expansion of vitality. In the evening, the number drops to 23 (5.67%), primarily located in major commercial centers. Over the course of the entire day, 31 station areas (7.65%) maintain high or medium-high vitality. Further local spatial

autocorrelation analysis reveals that hotspot areas (118 stations, 29.14%) are highly clustered within the central urban districts, whereas coldspot areas (110 stations, 27.16%) are mainly located in peripheral zones and newly developed areas. This reflects a pronounced spatial polarization pattern between the two.

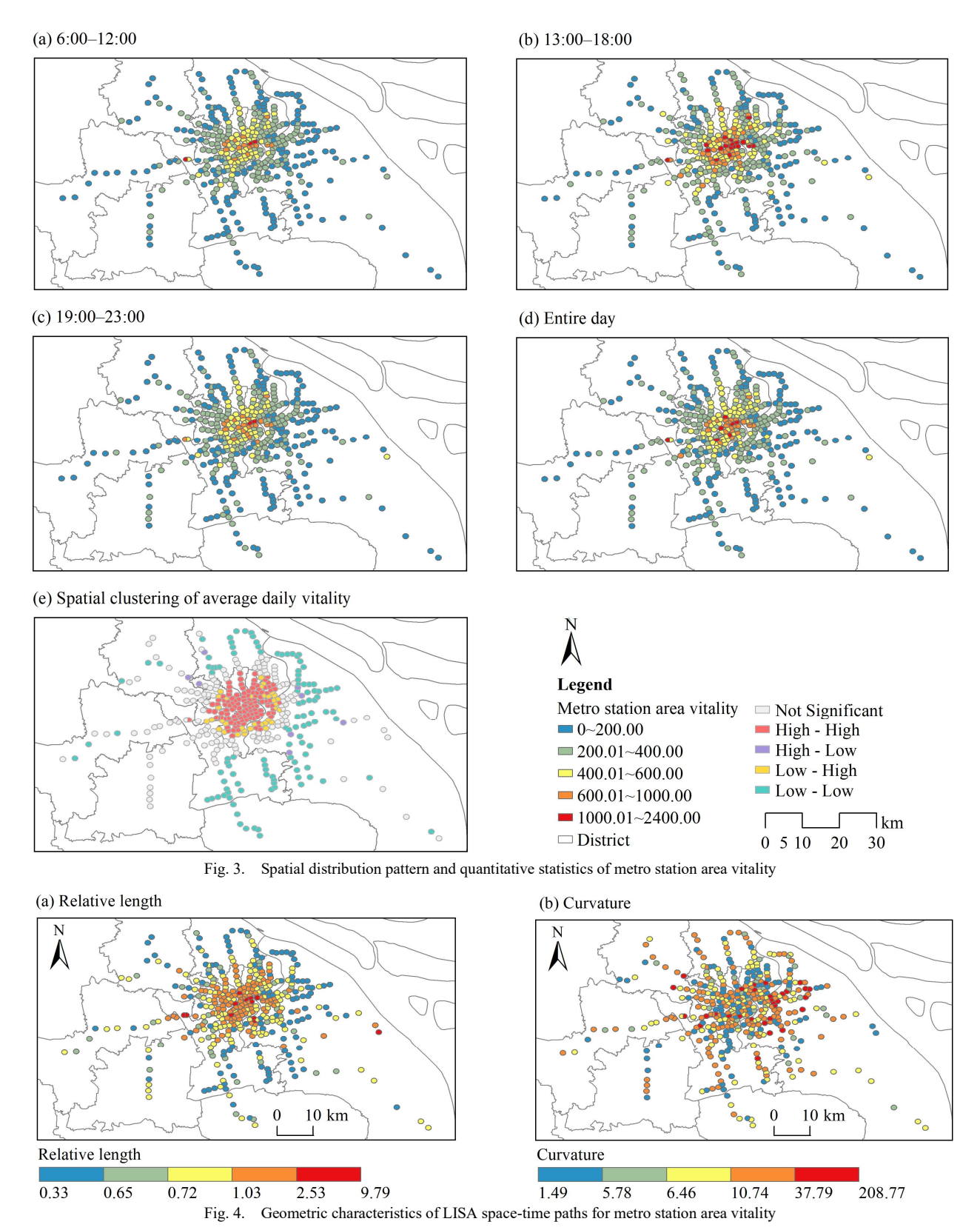
A.2. Spatiotemporal Dynamic Characteristics

To further characterize the dynamic patterns of metro station area vitality, this study applies LISA time path analysis, classifying both the relative length and curvature of the time paths into five levels using the natural breaks method in ArcGIS 10.8 (Figure 4).

The relative length of LISA time paths shows a concentric "core-periphery" decreasing pattern. The average relative length is 1, and 279 station areas (accounting for 68.89% of all stations) have a value below 1, indicating that the local spatial structure of vitality across most metro station areas in Shanghai is relatively stable. High values are mainly concentrated in the following four types of areas: (1) Core commercial zones, such as East Nanjing Road (6.13), People's Square (4.60), and Lujiazui (3.78). (2) Cultural and leisure areas, such as China Art Museum (9.79), Yuyuan Garden (4.35), and the National Exhibition and Convention Center (1.91). (3) Major transportation hubs, such as Hongqiao Railway Station (4.64), Pudong International Airport (3.38), and Shanghai Railway Station (3.47). (4) Key transfer nodes, such as Century Avenue (2.52), Yaohua Road (2.83), and Zhongshan Park (1.92). These areas exhibit strong dynamism due to their multifunctional roles, accessibility, and strong passenger flow aggregation effects.

The curvature presents a spatial pattern of "scattered large dispersion, clustered small aggregation." The average bending degree is 15.68, with 106 station areas (26.17%) exceeding this value. High values demonstrate the following four characteristics: (1) Sporadic distribution in peripheral or newly developed areas, such as Jiangyue Road (208.77), Nanxiang (46.32), and Fengbin (40.93). (2) Concentration around functional hubs or tourist attractions, such as China Art Museum (182.41), Hongqiao Airport (72.91), and Disneyland (34.27). (3) Few high values in the city center, though some dense transfer zones still show high degrees, such as Minsheng Road (117.24), Siping Road (89.70), and Yanggao Middle Road (69.34). (4) Mostly located in transitional zones on the edge of central districts, serving as important connectors between urban and suburban areas, such as Guanglan Road (148.19), Pusan Road (98.84), and Jinji Road (94.93). These areas experience substantial fluctuations in spatial dependence of vitality, with spillover effects from neighboring areas playing a particularly significant role.

Notably, 39 metro station areas (9.63%) simultaneously exceed the average values for both relative length and curvature, including the China Art Museum, Oriental Sports Center, and Lujiazui. These locations frequently host large-scale public events or experience surges in passenger volume during holidays, rendering them susceptible to abrupt fluctuations in vitality that may affect traffic stability and spatial order. Consequently, it is imperative to implement real-time dynamic monitoring and early warning systems to accurately detect variations in passenger flow and to strengthen emergency response and regulatory capacity, thereby ensuring the efficient and orderly operation of these station areas.



Based on the spatial coordinates derived from the Moran's I scatterplot of metro station area vitality, a spatiotemporal transition probability matrix was constructed (Table IV). The results reveal that among the four types of spatiotemporal transition patterns, Type IV transitions dominate, with transition probabilities exceeding 85% across all cases. This indicates a strong path dependence in metro station area vitality in Shanghai during weekends, and reflects a spatial structure characterized by significant inertia and lock-in effects. Meanwhile, although the probabilities of other transition types are relatively low, they still reflect

localized changes in vitality status: Type I transitions primarily include $LH_t \rightarrow HH_{t+1}$ (6.78%) and $HL_t \rightarrow LL_{t+1}$ (10.71%). Type II transitions are mainly observed in $LH_t \rightarrow LL_{t+1}$ (2.99%) and $HL_t \rightarrow HH_{t+1}$ (2.47%). Type III transitions are extremely rare, with only $HL_t \rightarrow LH_{t+1}$ (0.82%), indicating that synchronous vitality changes between a station and its neighbors are uncommon. Overall, the vitality of metro station areas in Shanghai exhibits a typical "Matthew Effect": high-vitality areas are more likely to maintain their dominant positions, while low-vitality areas struggle to break out of the existing pattern.

B. Driving Force Analysis of Metro Station Area Vitality

Based on the GD package in R, this study constructs an optimal-parameter geographical detector model. Continuous data are discretized using a combination of the natural breaks method, geometrical interval, equal interval, quantile, and standard deviation methods, with the number of categories set between 3 and 10. The optimal parameter combination is determined based on the maximization of the q-statistic. A ranking analysis of the q-values for the four time periods—6:00–12:00, 13:00–18:00, 19:00–23:00, and the entire day—is conducted (Table V). The q-values of all built environment variables passes the 1% significance level, indicating that these variables significantly influence the spatial differentiation of metro station area vitality.

Across all time periods, the following eight factors consistently rank in the top positions in terms of explanatory power: density of commercial service facilities, density of leisure and entertainment facilities, distance to the city center, density of educational and cultural facilities, closeness centrality, density of business office facilities, sky visibility, and floor area ratio. Their q-values range from 0.43 to 0.75, showing strong temporal stability. Among them, the densities of commercial service and leisure and

entertainment facilities consistently occupy the top two positions, both with q-values above 0.58, suggesting that commercial activity and leisure consumption are the dominant driving forces behind metro station area vitality. Notably, these two variables peak in explanatory power during the afternoon period, aligning well with citizens' behavioral patterns of leisure, socializing, and shopping during weekend afternoons. In addition, the densities of educational, cultural, and office facilities also demonstrate strong explanatory power, reflecting ongoing educational and work-related demands even on weekends in Shanghai. Furthermore, the importance of distance to the city center, closeness centrality, sky openness, and floor area ratio confirms the fundamental role of location advantages and urban spatial form in shaping vitality. In contrast, the explanatory power of street green view index and visual entropy is relatively limited, with q-values below 0.2, indicating that pedestrians' perception of fine-grained environmental details around metro station areas is relatively limited. This may be because broader spatial factors exert a stronger influence on vitality than localized environmental perceptions at the pedestrian scale.

TABLE IV
SPATIOTEMPORAL TRANSITION PROBABILITY MATRIX OF METRO STATION AREA VITALITY

t/t+1 HH_{t+1} LH_{t+1} LL_{t+1} HH. TYPE IV(0.9569) TYPE II(0.0050) TYPE I(0.0381) TYPE III(0) HL_t TYPE II(0.0247) TYPE IV(0.8600) TYPE III(0.0082) TYPE I(0.1071) LH_t TYPE I(0.0678) TYPE III(0) TYPE IV(0.9023) TYPE II(0.0299) TYPE III(0) TYPE I(0.0147) TYPE II(0.0108) TYPE IV(0.9745) LL.

 $\label{table v} TABLE\ V$ Detection results of vitality driving factors in Subway station areas

Dimension	D:: E 4	6:00-12:00		13:00-18:00		19:00-23:00		Entire Day	
Dimension	Driving Factor	q-value	Rank	q-value	Rank	q-value	Rank	q-value	Rank
Land use intensity	Floor area $ratio(X_1)$	0.464	8	0.461	7	0.434	9	0.465	8
	Functional $mix(X_2)$	0.330	13	0.258	15	0.293	13	0.295	13
Population and facility distribution	Resident population density(X_3)	0.331	12	0.251	16	0.301	12	0.292	14
	Commercial service facility density(X_4)	0.670	1	0.749	1	0.687	1	0.723	1
	Business and office facility density(X_5)	0.473	7	0.531	4	0.470	7	0.506	6
	Educational and cultural facility density(X_6)	0.524	4	0.530	5	0.491	4	0.528	4
	Leisure and entertainment facility density(X_7)	0.586	2	0.691	2	0.607	2	0.644	2
	Bus stop density(X_8)	0.410	10	0.444	9	0.439	8	0.441	9
Transportation	Road density(X_9)	0.422	9	0.397	11	0.388	10	0.407	11
and accessibility	Street betweenness(X_{10})	0.382	11	0.438	10	0.371	11	0.412	10
	Distance to city center(X_{11})	0.537	3	0.556	3	0.494	3	0.544	3
	Distance to tertiary $hospital(X_{12})$	0.285	15	0.238	17	0.221	18	0.254	17
Street environmental quality	Green view index(X_{13})	0.118	19	0.115	19	0.141	19	0.124	19
	Street safety index(X_{14})	0.252	18	0.200	18	0.223	17	0.227	18
	Sky openness(X_{15})	0.487	6	0.460	8	0.483	5	0.476	7
	Street visual entropy(X_{16})	0.048	20	0.039	20	0.047	20	0.044	20
Metro station characteristics	Closeness centrality(X_{17})	0.524	5	0.521	6	0.471	6	0.519	5
	Betweenness centrality(X_{18})	0.282	16	0.293	14	0.250	15	0.279	16
	Metro station age(X_{19})	0.311	14	0.325	12	0.271	14	0.309	12
	Number of entrances/exits(X_{20})	0.264	17	0.318	13	0.236	16	0.285	15

The interaction detection results (Figure 5) indicate that the effects of various built environment factors on metro station area vitality are interdependent rather than isolated. Most factor combinations exhibit bivariate or nonlinear enhancement, while only a few display univariate nonlinear weakening, suggesting that metro station area vitality arises from the synergistic and combined influence of multiple interacting factors.

Across different time periods, the density of commercial service facilities shows the strongest interactive explanatory power when combined with distance to the city center, floor area ratio, bus stop density, and the densities of educational and cultural facilities, with q-values all exceeding 0.78. Additionally, interactions involving business office, educational, cultural, and leisure facility densities with bus stop density and closeness centrality demonstrate strong explanatory power, with q-values consistently above 0.6. This highlights the critical importance of coordinated spatial layout and the effective integration of public transport systems with multifunctional facilities. Further analysis reveals that the interactive explanatory power of most factors increases during weekend afternoons, when travel demand rises, suggesting that frequent activity scenarios help to strengthen the interactions among built environment factors. Compared with single-factor interaction results, the explanatory power of street green view index and visual entropy improves significantly when interacting with other factors, with some showing nonlinear enhancement effects, indicating that the influence of street-level environmental elements tends to emerge under compound conditions.

C. The Spatiotemporal Driving Mechanism of Built Environment Factors on Metro Station Area Vibrancy

To further examine the spatiotemporal heterogeneity in the effects of built environment factors on metro station area vibrancy, twelve indicators with the highest average explanatory power identified through the Geodetector analysis were selected: X_1 , X_2 , X_4 , X_5 , X_6 , X_7 , X_8 , X_9 , X_{10} , X_{11} , X_{15} , and X_{17} .

Considering the sensitivity of the GTWR model to variable scales, both independent and dependent variables were standardized prior to modeling. As presented in Table VI, the GTWR model outperforms the OLS, GWR, and TWR models, exhibiting a notably higher R^2 value and lower AICc and RSS values. These results underscore the superior performance of GTWR in capturing the spatiotemporal non-stationarity inherent in metro station area vibrancy.

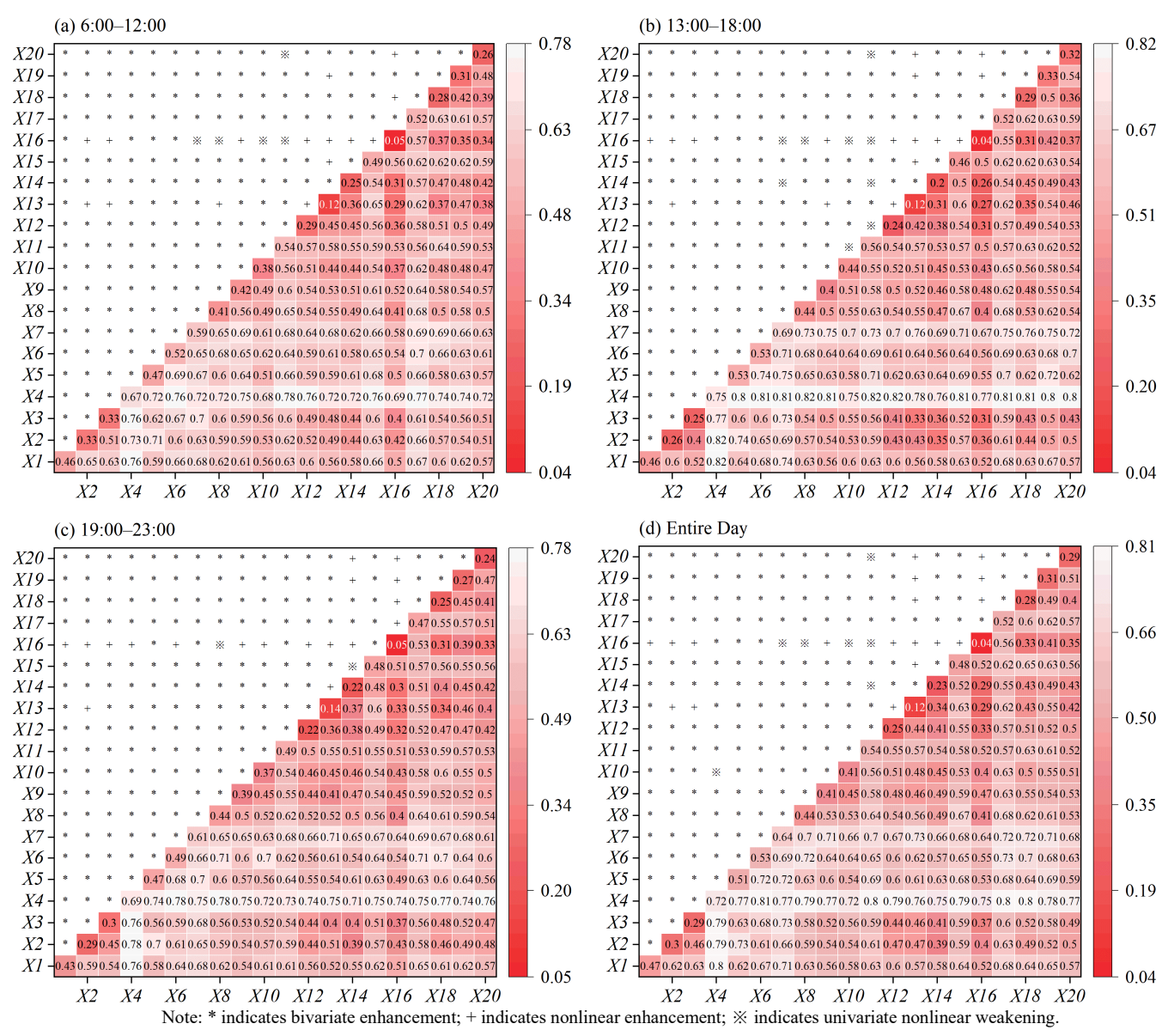


Fig. 5. Interaction analysis results of driving factors for subway station area vitality

I ABLE VI	
OMPARISON OF MODEL RESULTS	

COMI ARISON OF MODEL RESCETS						
Model	R^2	AICc	RSS			
OLS	0.65	12813.69	2472.03			
GWR	0.74	11351.91	1856.79			
TWR	0.84	7489.92	1143.59			
GTWR	0.89	5534.29	805.12			

As illustrated in Figure 6, the regression coefficients of built environment variables in the GTWR model exhibit considerable variation, with most factors exerting both positive and negative effects across space and time. Notably, variables such as distance to the city center, street connectivity, closeness centrality, educational and cultural facility density, and land-use mix demonstrate substantial fluctuations in their coefficients, reflecting a high degree of spatiotemporal heterogeneity in their influence on metro station-area vibrancy. In contrast, bus stop density and road density display more narrowly distributed coefficients with limited variation, indicating a relatively stable and consistent effect of public transit accessibility and road infrastructure. These findings underscore the differentiated roles of built environment components in shaping station-area vibrancy and emphasize the need for context-sensitive planning strategies that account for local spatial and temporal dynamics.

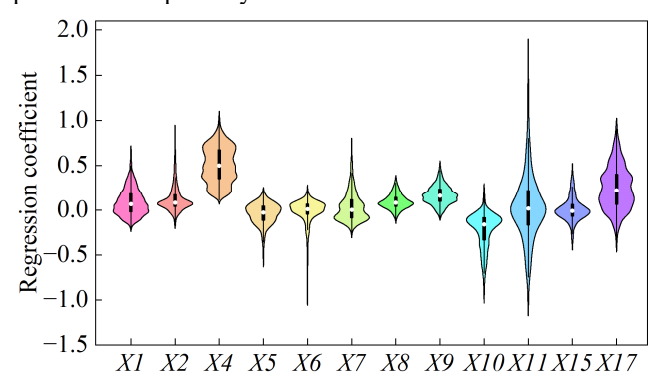


Fig. 6. Violin plot of GTWR regression coefficients for built environment variables

C.1. Temporal Heterogeneity of Built Environment Effects

Plotting the curves of average GTWR regression coefficients for each built environment variable across different time periods helps to capture the dynamic changes in their overall influence intensity and direction (Figure 7).

At the land use level, the positive impact of floor area ratio shows a steady upward trend overall, indicating that areas with higher development intensity can continuously stimulate station-area vibrancy and play a crucial role in promoting the nighttime economy and sustaining urban vitality. The influence of functional mix on metro station-area vibrancy exhibits a "double-peaked" pattern, with two distinct peaks at 10:00 and 19:00. From 6:00 to 10:00, as residents begin commuting and morning activities unfold, areas with higher functional mix are more likely to stimulate diverse behavioral demands, thereby enhancing vibrancy. Between 10:00 and 15:00, its influence weakens, possibly due to dispersed population activity and stabilized functional needs during midday. From 15:00 to 19:00, the positive effect strengthens again, but declines after 20:00 as indicated by a drop in regression coefficients.

At the level of functional facilities, the positive impact of commercial service facility density shows a continuous upward trend during the daytime. After 19:00, this positive effect begins to weaken, likely due to the reduction of nighttime commercial activities and declining consumer demand. The density of office facilities exerts a consistently negative impact throughout the day. Between 6:00 and 9:00, this negative effect gradually weakens, indicating that some enterprises in Shanghai remain operational during the weekend morning peak, generating a certain level of foot traffic. After 14:00, the negative impact significantly intensifies, revealing the "vacancy" characteristic of office functions on non-working days and its constraining effect on urban vitality. The negative influence of science, education, and cultural facility density weakens gradually from 6:00 to 15:00, reflecting daytime demand from citizens for exhibitions, family education, and cultural leisure activities on weekends. After 18:00, the negative effect increases rapidly, mainly due to the limited opening hours and functional attributes of such venues. The density of leisure and entertainment facilities suppresses station-area vibrancy between 6:00 and 9:00, as most of these venues are not yet open and fail to attract foot traffic. After 10:00, the regression coefficient shifts from negative to positive and peaks in the afternoon, indicating strong attraction during the midday to evening hours. After 20:00, the coefficient declines again and gradually turns negative.

At the transportation and locational level, both bus stop density and road density exhibit a "rise-then-fall" pattern in their positive influence. The impact of bus stop density on station-area vibrancy peaks around midday; although the regression coefficient fluctuates slightly afterward, it remains at a relatively high level overall, indicating that bus accessibility continuously supports vibrancy. Road density is more effective in enhancing pedestrian aggregation during morning travel periods, but its influence significantly weakens in the evening. The regression coefficient of street connectivity follows a "W-shaped" trend. On the one hand, during the two peak travel periods (6:00-10:00 and 15:00–19:00), the negative effect becomes more pronounced. This is because streets with high connectivity, serving as arterial corridors in the traffic network, tend to facilitate rapid movement and dispersal of people, thereby diluting the concentration of vibrancy in metro station areas. On the other hand, during non-peak periods (11:00-14:00 and 20:00-23:00), the negative influence is relatively weaker, suggesting a lower degree of street network intervention in organizing pedestrian flows in metro areas. The effect of distance to the city center can be divided into three phases. From 6:00 to 10:00, the regression coefficient is negative, reflecting a "centripetal" pattern of morning activities. Between 10:00 and 19:00, the coefficient turns positive and increases steadily. showing a clear trend "decentralization." After 19:00, the coefficient drops sharply and turns negative again after 21:00, indicating that nighttime activities become re-concentrated in central urban areas.

At the level of street spatial form, sky openness exhibits a negative regression coefficient between 6:00 and 10:00, suggesting that people in the morning prefer street environments with enclosure and a sense of shelter. As time progresses, the coefficient shifts from negative to positive, reflecting an increasing preference for open and sunlit outdoor environments in the afternoon. After 19:00, the coefficient turns negative again, indicating that open spaces lose their attractiveness at night—likely due to reduced

perceived safety and increased potential crime risk. This makes people more inclined to choose streets with continuous interfaces, clear spatial boundaries, and vibrant or community-oriented atmospheres to meet their needs for socializing, relaxation, and emotional belonging.

At the metro network level, the regression coefficient of closeness centrality exhibits an inverted "U-shaped" temporal trend. From 6:00 to 12:00, its positive effect rises sharply, underscoring the critical role of highly central stations in stimulating vibrancy during the morning hours. Between 13:00 and 18:00, the coefficient remains elevated, reflecting the continued ability of these stations to attract cross-regional flows and strengthen the spatial coupling between metro network topology and human mobility. After 18:00, the influence diminishes, likely due to a shift in travel behavior—from daytime, function-driven inter-district trips to more localized, point-to-point return-home movements.

Collectively, these temporal patterns underscore the complex, dynamic, and context-dependent ways in which built environment elements influence metro station-area vibrancy. They highlight the critical need for planning strategies that are temporally responsive, functionally targeted, and spatially adaptive to effectively support sustainable and resilient urban vitality.

C.2. Spatial Heterogeneity of Built Environment Effects

Based on the analysis results in Figure 6, one to two built environment variables exhibiting notable spatial heterogeneity are selected from each dimension as representative indicators. These variables are then used to visualize the spatial distribution of average GTWR regression coefficients across different station areas (Figure 8). This visualization highlights the varying influence of key built environment factors on station-area vibrancy, offering insights into their localized and context-dependent effects.

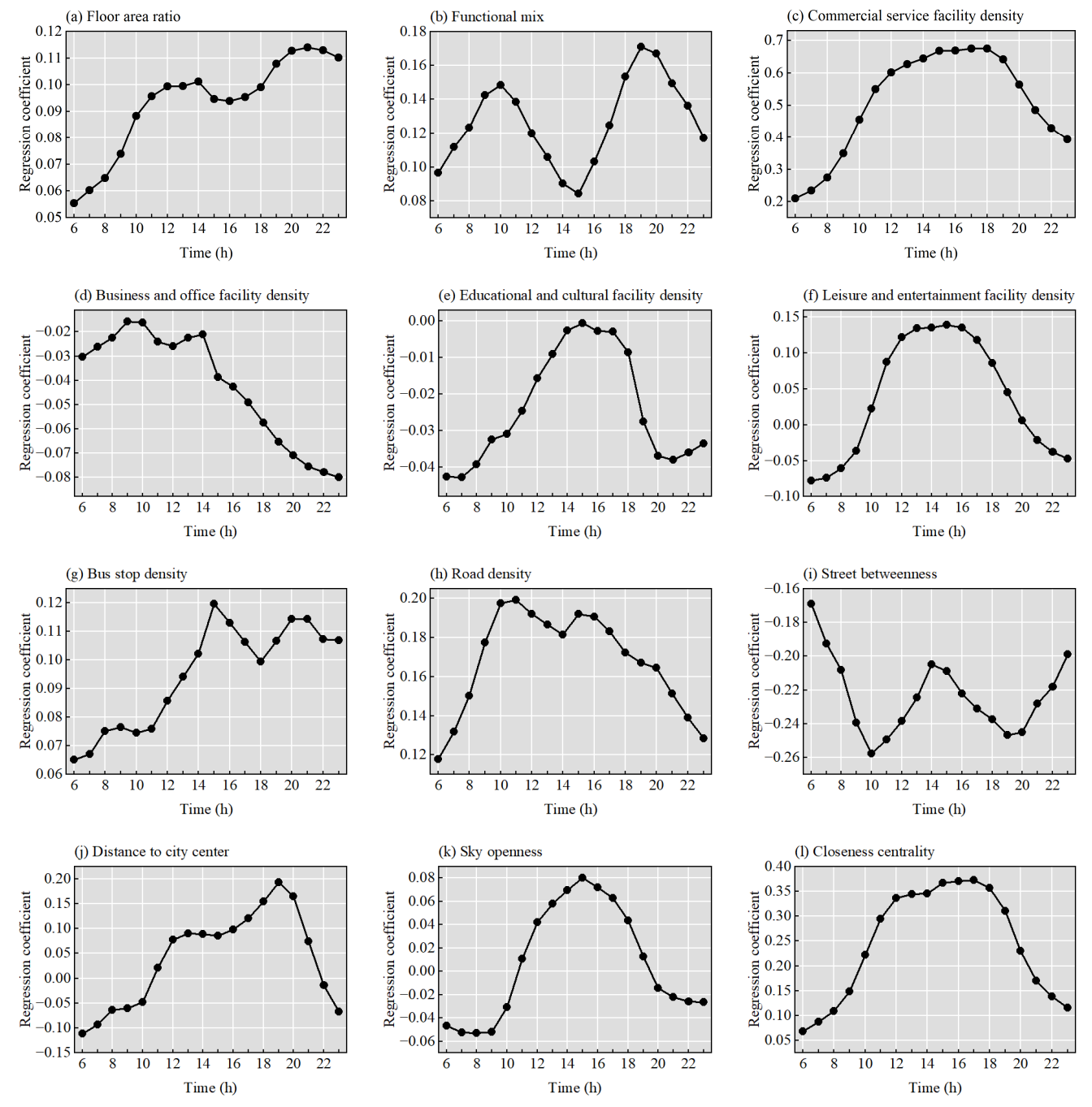


Fig. 7. Temporal heterogeneity of the impact of built environment factors on metro station area vitality

At the land use level, the impact of floor area ratio exhibits a spatial pattern of being higher in the southwest and lower in the northeast. Station areas with strong positive effects are mainly located in the southern part of Pudong New Area, the Expo Zone, the riverside area of Pudong, and major transportation hubs. These areas are often situated in emerging zones of the city's development strategy, characterized by high demand for mixed functions, planning flexibility, and strong policy support—aligning well with the principles of TOD. In contrast, station areas with strong negative effects are primarily concentrated in the northeastern industrial belt of Pudong, the aging built-up areas of Puxi, and the mixed industrial-residential zones in Baoshan-Jiading in the north. Constrained by land-use regulations, high spatial renewal costs, and the need to preserve ecological and historical features, increasing development intensity in these areas is difficult to translate into substantial urban vitality. The influence of functional mix exhibits a "center - periphery" spatial pattern. Station areas with stronger positive effects are concentrated in the core area within the Inner Ring, which benefits from a rich historical legacy and a mature urban functional system, resulting in highly integrated and diverse functional characteristics. Conversely, station areas with stronger negative effects are mostly located in suburban new towns, terminal metro stations, and specialized industrial parks. These areas generally face structural issues such as mono-functional land use and lagging public service facilities, and their spatial vitality has yet to be fully activated.

At the level of functional facilities, the influence of the density of science, education, and cultural facilities exhibits a spatial pattern of being higher in the northeast and lower in the southwest. Station areas with stronger positive effects are mainly concentrated in the Zhangjiang-Waigaoqiao corridor, the Hongkou-Yangpu area, and the riverside comprehensive service belt. These areas host a large number of universities and research institutions and benefit from the advantages of free trade zones, high-tech parks, and modern service industries, forming spatial carriers with a high degree of integration between knowledge concentration and innovation-driven development. In contrast, station areas with stronger negative effects are mostly located in the distant suburban new towns and around major transportation hubs, where issues such as a shortage of educational resources and low population density of knowledge workers are common. The impact of the density of leisure and entertainment facilities shows spatial a symmetrically distributed along a diagonal axis. Station areas with stronger positive effects are mainly located in the outer city areas of Jiading, Qingpu, and Pudong New Area. These areas host landmark leisure destinations such as Disneyland, the Wildlife Park, and ecological parks, which not only fill the entertainment service gap in the suburbs but also attract large numbers of external visitors due to their destination appeal, making them popular choices for weekend leisure and short-distance travel. Station areas with stronger negative effects are mainly distributed in the central urban area. Due to limited land resources, the addition of new leisure facilities may lead to a "functional crowding-out" effect, occupying space originally intended for community services or residential use, thereby weakening overall vitality.

At the level of transportation and location, the influence of street permeability exhibits an overall spatial pattern of being higher in the east and lower in the west. Station areas with stronger positive effects are mainly located in Xujiahui, the Expo-Qiantan area, Huangpu District, and Pudong New Area. These areas feature dense road networks and well-developed branch road systems, providing convenient access for pedestrians and non-motorized vehicles. Conversely, station areas with stronger negative effects are mainly situated around the Honggiao transportation hub. Songjiang, Qingpu, and Baoshan. These areas are often traversed by expressways and major arterial roads, leading to fragmented station area spaces and obstructed pedestrian and non-motorized travel. The impact of distance to the city center shows both strong positive and negative effects. Station areas with stronger positive effects are primarily concentrated in municipal-level commercial centers, the Hongqiao transportation hub, and the northern part of Jing'an District. This indicates that these areas have developed self-sustaining and mutually reinforcing functional ecosystems, demonstrating strong locational resilience and the capacity to attract foot traffic-further validating the necessity of promoting a polycentric urban structure. On the other hand, station areas with stronger negative effects are mainly distributed in suburban new towns, the Jinqiao-Waigaoqiao area, northern Yangpu District, and the central-western part of Pudong, which may be due to developmental gaps in their comprehensive service systems compared to the city center.

At the level of street spatial morphology, the influence of sky openness exhibits a spatial pattern of being higher in the central areas and lower in the periphery. Station areas with stronger positive effects are mostly concentrated in the core districts of Puxi, the Expo-Qiantan area, and Sanlin-Beicai. These areas feature well-developed pedestrian facilities and continuous, compact street interfaces. A moderate degree of sky openness helps enhance spatial permeability and visual comfort. Station areas with stronger negative effects are located in the Hongkou–Yangpu Qingpu-Jiading, and the far southern outskirts of Pudong. Although these areas have certain urban functions and population bases, they are often surrounded by large residential communities, gated campuses, or industrial parks. Some streets suffer from oversized spatial scales, weak interface organization, or monotonous frontage functions. The lack of commercial permeability and public activity support means that higher sky openness may instead intensify the sense of emptiness and detachment, thereby reducing the attractiveness of the station areas.

At the level of metro characteristics, the spatial distribution of the positive and negative effects of centrality proximity varies significantly. Station areas with stronger positive effects are mainly distributed in Songjiang, Xinzhuang, Hongqiao, Beicai, Chuansha, and along the northern section of Line 1. These areas are generally secondary urban centers or emerging development clusters, where improved metro accessibility has strengthened connections between the periphery and the urban core. In contrast, station areas with stronger negative effects are primarily found in Jinqiao-Waigaoqiao, Fengxian, northern Yangpu, and southern Minhang. These areas are often oriented toward industrial parks, logistics and warehousing, residential functions, and they tend to service-oriented and consumption-oriented facilities. Some

station areas also face problems related to inadequate "last-mile" transport connections, resulting in metro accessibility not translating into substantial foot traffic.

Overall, the spatial heterogeneity in the effects of built environment variables reflects the intricate interplay between urban function, spatial structure, and development stage, highlighting the need for differentiated and context-sensitive planning strategies to optimize metro station-area vibrancy across diverse urban settings.

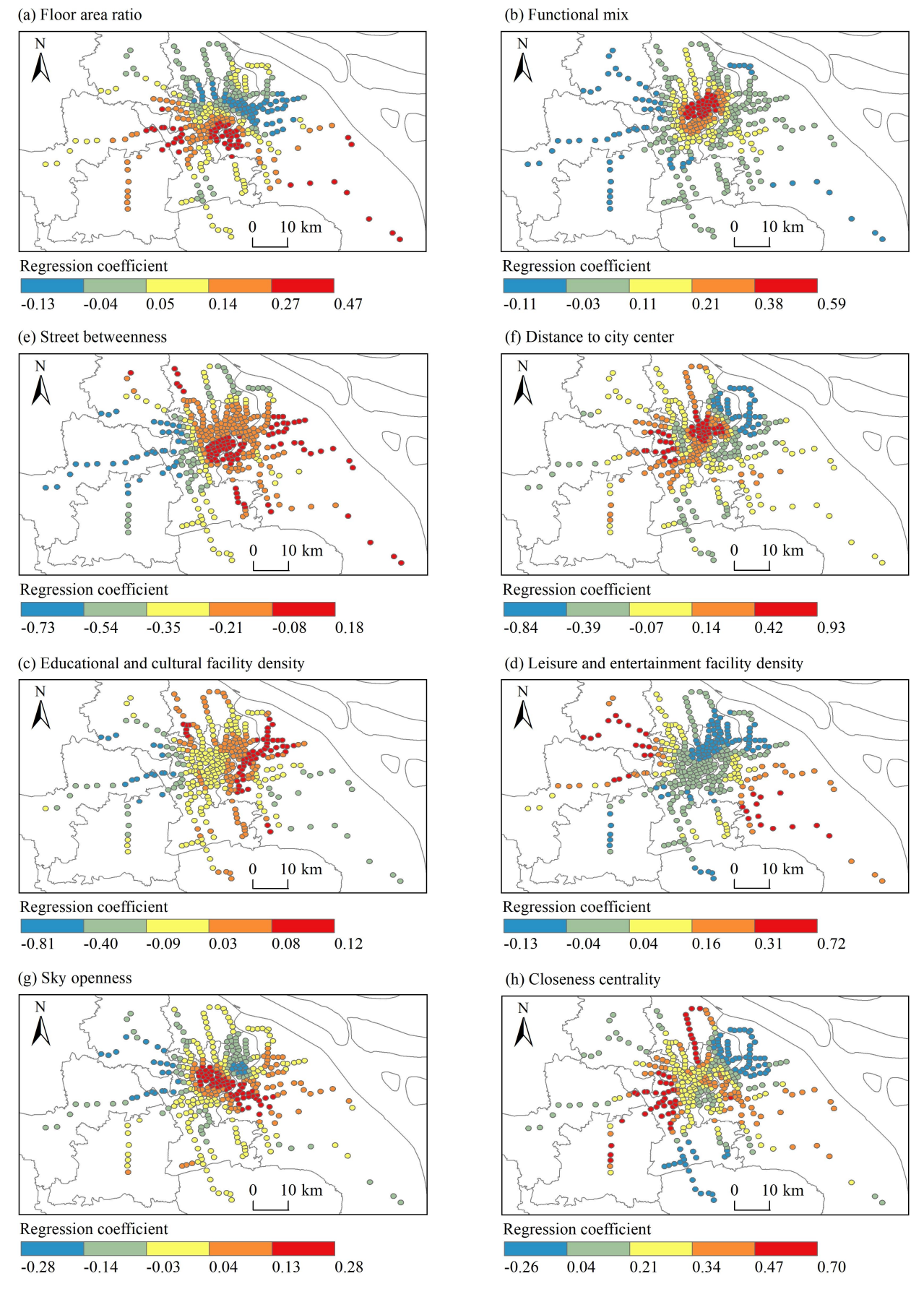


Fig.8 Spatial heterogeneity of the impact of built environment factors on metro station area vitality

D. Analysis of Typical Metro Station Areas

To further investigate the relationship between the built environment and metro station area vibrancy, six representative stations—People's Square, Xujiahui, China Art Museum, Jinqiao Road, Jiangyue Road, and Pujiang Town—were selected, covering a spectrum from the urban core to the outer fringe and representing varying levels of vibrancy. Case analyses based on urban functional layout and spatial morphology were conducted to uncover the differentiated mechanisms and underlying logic driving vibrancy across station types.

(1) People's Square

As one of Shanghai's most iconic central areas, the People's Square station area exhibits exceptionally high densities of commercial, cultural, and educational facilities. It ranks among the highest in the sample in terms of functional mix (0.74), cultural and educational facility density (121.12), recreational facility density (199.44), and street connectivity (43.14). These reflect a highly multifunctional and population-attracting environment. Serving as both an administrative hub and a major transportation node, this area demonstrates the amplification effect of a "monocentric core" on urban vibrancy and stands as a model for the vibrancy-driving potential of the built environment.

(2) Xujiahui

Located within the inner ring, Xujiahui serves as a vital secondary urban center. It features strong street connectivity (18.56), high development intensity (FAR: 4.22), a high degree of functional mix (0.75), and substantial recreational facility provision (96.95). With a mature commercial ecosystem and preserved historical neighborhoods, the area benefits from compact urban form and high connectivity, representing the combined effect of spatial structure and street quality in sustaining vibrancy.

(3) China Art Museum

Situated within the Expo Park zone, the China Art Museum station plays a key role in the Pudong riverside development belt. It boasts a high floor area ratio (4.21), with notable centrality and functional mix, highlighting the vibrancy potential of emerging functional zones under policy support and flexible development. Although its density of cultural and recreational facilities is lower than that of core areas, the presence of cultural landmarks, exhibition venues, and a composite spatial layout signal a transition from mono-functionality to comprehensive vibrancy, making it a representative of "planning-led" positive evolution.

(4) Jinqiao Road

Located in Pudong's traditional industrial belt, the Jinqiao Road station area shows relatively high functional mix (0.76), but suffers from low FAR (1.76) and limited recreational facility density (29.86). Its centrality and proximity to the city center are both moderate to low, indicating that metro accessibility has not effectively activated vibrancy in the area. It typifies areas in urban renewal where single-industry orientation and low development intensity hinder the release of spatial vitality, exposing a mismatch between the built environment and urban functions.

(5) Jiangyue Road

Jiangyue Road station is located on the outer edge of Minhang District. It ranks low in both cultural and educational facility density (13.27) and recreational facility density (13.78). While the sky openness is relatively high (0.25), street connectivity remains poor (9.20), forming a typical "high openness—low accessibility" pattern. The overly wide street interfaces limit pedestrian aggregation and lack adequate service penetration, resulting in persistently low vibrancy. This highlights the structural design challenges in low-density residential areas at the urban fringe.

(6) Pujiang Town

As a suburban station in southern Pudong, Pujiang Town ranks among the lowest across several built environment indicators, particularly in cultural and educational facility density (9.45) and centrality (0.065). This reflects deficiencies in knowledge-intensive resources and poor travel connectivity. The area exemplifies the structural low vibrancy caused by jobs-housing imbalance and lagging infrastructure provision—a "static zone" shaped by the spatial mismatch between metro benefits and land use.

E. Built Environment Driving Mechanisms Analysis

Spatial regression of built environment elements and the case analysis of typical station areas reveal that the generation of metro station area vibrancy is not only influenced by physical spatial attributes but also reflects a deeper coupling of various mechanisms, including urban functional organization, travel behavior preferences, and the regional job-housing structure. This coupling is particularly evident during weekends, when commuting demand subsides and residents' mobility shifts toward consumption, leisure, and social activities. Consequently, station area vibrancy becomes more dependent on environmental perception and functional provision, amplifying the spatial and temporal heterogeneity of built environment effects.

From the perspective of metro service functionality, a station's hierarchical position within the urban transit network significantly affects its vibrancy level. Central hubs such as People's Square and Xujiahui, with superior network connectivity and transfer capacities, serve as major population convergence nodes, exhibiting substantially higher vibrancy than peripheral stations. In contrast, stations located at terminal points or suburban edges often suffer from limited coverage and weak "last-mile" connectivity. Despite some degree of built-up intensity, these areas fail to effectively attract pedestrian flow and activity.

From a travel behavior perspective, weekend mobility is characterized by a high degree of self-organization and purpose-driven activity. Residents tend to gravitate toward areas with a high concentration of cultural, recreational, and commercial functions, reflecting a strong preference for "experiential spaces." This accounts for the heightened vibrancy observed in station areas with abundant cultural-tourism amenities and well-integrated functions, while those marked by pronounced job-housing separation and functional singularity often exhibit a disconnect between physical form and perceived vitality—manifesting as "visible structure, invisible vibrancy."

From the perspective of job-housing spatial structure, differences in the degree of functional integration and spatial positioning among station areas represent a key mechanism behind vibrancy disparities. Central urban zones generally maintain better job-housing balance and higher functional density, sustaining strong flows of people and activity even on weekends. In contrast, areas such as

industrial parks or mono-functional residential zones, where functional fragmentation is severe, often struggle to meet diverse weekend needs, despite favorable accessibility or development intensity.

IV. CONCLUSION AND DISCUSSION

A. Conclusion

This study focuses on the vibrancy of metro station areas in Shanghai during weekends. By applying an Exploratory Spatiotemporal Data Analysis framework, it characterizes the dynamic variations of station-area vibrancy. Building on this, the study further employs the Optimal Parameter-based Geographical Detector and the Spatiotemporal Geographically Weighted Regression model to explore the driving mechanisms of built environment factors. The main conclusions are as follows:

- (1) Metro station area vibrancy in Shanghai exhibits significant positive spatial autocorrelation and clear spatiotemporal differentiation. Temporally, vibrancy intensity follows a trend of "increase—stabilization—decline," while the degree of spatial agglomeration undergoes a process of "enhance—weaken—re-enhance." Spatially, the overall structure of vibrancy is characterized by a compound pattern of "core radiation + axial extension." Hotspots are concentrated in central urban areas, while coldspots are mainly located in the urban periphery and newly developed zones, indicating a pronounced spatial polarization.
- (2) The local spatial structure of metro station-area vibrancy demonstrates high stability. Stations with high relative lengths of LISA time paths are primarily located in core business districts, cultural and recreational zones, major transportation hubs, and key transfer nodes. Stations with high curvature of LISA time paths are mostly found in transitional belts at the edge of the central city, functional hubs, and scenic spots, scattered across the urban periphery and transfer-intensive zones. The spatiotemporal evolution of vibrancy is marked by strong path dependence and spatial lock-in, reflecting a typical "Matthew effect", where spontaneous breakthroughs or transformations are difficult to achieve.
- (3) Factor detection results indicate that the key determinants of metro station-area vibrancy include: commercial service facility density, recreational facility density, distance to the city center, educational and cultural facility density, closeness centrality, office facility density, sky openness, and floor area ratio. In contrast, green view index and visual entropy exhibit relatively weak explanatory power. Interaction detection further reveals that under conditions of frequent activity, the interactions among built environment factors become more pronounced. Specifically, commercial service facility density shows the strongest interactional explanatory power with distance to the city floor area ratio, bus stop density, and educational/cultural facility density across different time periods. In comparison, the impact of street-level environmental features tends to rely on multi-factorial conditions to be effective.
- (4) The influence of built environment elements on station-area vibrancy exhibits notable spatiotemporal heterogeneity, with most variables showing both positive and negative effects. Variables such as distance to the city center, street permeability, closeness centrality,

educational/cultural facility density, and land-use mix demonstrate strong spatiotemporal dependence in their influence across different station areas. In contrast, bus stop density and road density have relatively stable impacts on vibrancy.

B. Policy Implications

Based on the research findings, several planning recommendations are proposed to enhance metro station-area vibrancy and support sustainable urban development. These recommendations aim to address the observed spatiotemporal and spatial heterogeneity of built environment influences, and to guide context-specific, evidence-based interventions in urban planning practice:

- (1) For the 39 station areas exhibiting significant vitality fluctuations, priority should be given to establishing dynamic sensing and emergency coordination mechanisms. By leveraging big data and intelligent sensing technologies, a real-time passenger flow monitoring and early warning system should be developed to enable accurate identification and rapid response to sudden crowd surges. Furthermore, hierarchical management strategies and contingency plans should be formulated based on spatial carrying capacity and the characteristics of specific events, thereby enhancing the emergency responsiveness and operational resilience of highly sensitive station areas during holidays and major public gatherings.
- (2) The spatial layout of commercial and recreational facilities should be optimized as a key driver to stimulate deeper vitality within station areas. It is essential to promote the integrated planning of public transportation systems and multifunctional facilities, strengthening the efficient linkage between transport networks and service functions. Street spaces should be organically integrated with surrounding built environment elements, and designed to be functionally mixed, pedestrian-friendly, and connected to slow-traffic systems, thus fostering high-quality public spaces with strong interactivity and experiential appeal. On the policy level, travel patterns and activity rhythms of residents across different time periods should be dynamically monitored, shifting spatial governance strategies from "static planning" to "temporal optimization."
- (3) For peripheral station areas with persistently low vitality, efforts should focus on the introduction of mixed-use functions and the provision of high-quality public services to revitalize local life. The introduction of high-frequency livelihood services—such as education, cultural and creative industries, healthcare, and community commerce—should be encouraged to create vibrant spaces aligned with local population structures and time-specific needs. By redeveloping idle land and underutilized spaces, the transformation of station areas from mere "rail access points" to vibrant "living hubs" can be realized, thus preventing the dual challenge of "railway isolation" and "vitality hollowing."
- (4) In core areas characterized by high population density and functional intensity, scientific management of functional coordination and capacity thresholds should be prioritized. While maintaining the advantages of agglomeration, adaptive strategies for regulating crowd capacity and functional allocation must be implemented to mitigate systemic risks stemming from resource overconcentration. Differentiated policy interventions and quality-oriented resource optimization should be employed to promote

functional complementarity and vitality spillovers between central urban areas and peripheral sub-centers. This will support the development of a polycentric, multi-level, and networked urban spatial structure, ensuring balanced vitality distribution and orderly spatial expansion.

C. Discussion

The strengths and contributions of this study are reflected in the following four aspects:

- (1) Compared with existing research, this study incorporates street-level environmental perception and metro station attributes into the analysis, thereby expanding and refining the conventional "5D" built environment framework. This allows for a more systematic and comprehensive assessment of metro station area vibrancy.
- (2) Building upon previous urban vibrancy studies, this research innovatively introduces an exploratory spatiotemporal data analysis framework that integrates temporal dynamics with local spatial dependence. By moving beyond the traditional static perspective, it enables a continuous representation of vibrancy from "momentary scenes" to "interactive dynamic scenarios," thereby advancing both the theoretical lens and technical approach in urban vibrancy research.
- (3) The study applies an optimal-parameter geographical detector to identify key driving factors and their interaction effects on metro station area vibrancy, effectively addressing the limitations of traditional detectors in parameter discretization and improving the reliability and robustness of the results. In factor detection, the temporal variations in the explanatory power of built environment elements help clarify the phased priorities and intervention opportunities for regulating station area vibrancy. In interaction detection, the study fills a gap in previous research by addressing the insufficient attention to complex interaction mechanisms, offering a theoretical foundation for coordinated interventions and systematic enhancements of station area vibrancy.
- (4) By integrating the Geographically and Temporally Weighted Regression (GTWR) model, the study further reveals the spatiotemporal heterogeneity in the influence of built environment factors. Compared to OLS, GWR, MGWR, and conventional machine learning models, GTWR captures the spatiotemporal non-stationarity of variables more effectively, providing a more targeted methodological and practical basis for place-specific and time-sensitive urban spatial governance strategies.

Nevertheless, this study has several limitations that warrant further investigation. First, although Baidu's population heatmap data effectively captures the overall spatial patterns of population activity, it may be influenced by platform-specific behavioral biases and, therefore, may not fully reflect the vibrancy characteristics of diverse demographic groups. Second, as the analysis is confined to Shanghai as a case study, the temporal and spatial generalizability of the findings remains to be validated across cities with varying characteristics, in order to ascertain the broader applicability and limitations of the proposed analytical framework. Despite these limitations, the study establishes a systematic theoretical framework and provides empirical evidence for understanding the spatiotemporal driving mechanisms of built environment

factors on metro station-area vibrancy, offering meaningful insights for future research in this domain.

REFERENCES

- [1] J. Cui, J. D. Nelson, M. Beecroft, et al., "Subway systems and tourism: An overview and implications," Research in Transportation Business & Management, vol. 57, p. 101205, 2024.
- [2] Z. Yu, X. Zhu, and X. Liu, "Characterizing metro stations via urban function: Thematic evidence from transit-oriented development (TOD) in Hong Kong," Journal of Transport Geography, vol. 99, p. 103299, 2022.
- [3] Y. Fang, L. Zhao, K. Gu, et al., "Measuring the correlation between spatial vitality of metro station domain and built up environment in the main urban area of Hefei based on random forest model," Scientia Geographica Sinica, vol. 44, no. 5, pp. 796-807, 2024.
 [4] L. Wang, L. Hu, and X. Tian, "Multidimensional evaluation and
- [4] L. Wang, L. Hu, and X. Tian, "Multidimensional evaluation and spatiotemporal characteristics of metro station domain vitality based on big data: A case study of Xi'an City," Progress in Geography, vol. 42, no. 6, pp. 1112-1123, 2023.
- [5] X. Li, Y. Li, T. Jia, et al., "The six dimensions of built environment on urban vitality: Fusion evidence from multi-source data," Cities, vol. 121, p. 103482, 2022.
- [6] J. Yang, J. Cao, and Y. Zhou, "Elaborating non-linear associations and synergies of subway access and land uses with urban vitality in Shenzhen," Transportation Research Part A: Policy and Practice, vol. 144, pp. 74-88, 2021.
- [7] J. Montgomery, "Making a city: urbanity, vitality and urban design," Journal of Urban Design, vol. 3, no. 1, pp. 93-116, 1998.
- [8] S. Z. Zarin, M. Niroomand, and A. A. Heidari, "Physical and social aspects of vitality case study: Traditional street and modern street in Tehran," Procedia-Social and Behavioral Sciences, vol. 170, pp. 659-668, 2015.
- [9] D. I. Azmi and H. A. Karim, "Implications of walkability towards promoting sustainable urban neighbourhood," Procedia-Social and Behavioral Sciences, vol. 50, pp. 204-213, 2012.
 [10] F. Gao, X. Deng, S. Liao, et al., "Portraying business district vibrancy
- [10] F. Gao, X. Deng, S. Liao, et al., "Portraying business district vibrancy with mobile phone data and optimal parameters-based geographical detector model," Sustainable Cities and Society, vol. 96, p. 104635, 2023.
- [11] M. Chen, Y. Cai, S. Guo, et al., "Evaluating implied urban nature vitality in San Francisco: An interdisciplinary approach combining census data, street view images, and social media analysis," Urban Forestry & Urban Greening, vol. 95, p. 128289, 2024.
- [12] C. Wu, Y. Ye, F. Gao, et al., "Using street view images to examine the association between human perceptions of locale and urban vitality in Shenzhen, China," Sustainable Cities and Society, vol. 88, p. 104291, 2023.
- [13] R. Cervero and J. Day, "Suburbanization and transit-oriented development in China," Transport Policy, vol. 15, no. 5, pp. 315-323, 2008.
- [14] R. Ewing and R. Cervero, "Travel and the built environment: A meta-analysis," Journal of the American Planning Association, vol. 76, no. 3, pp. 265-294, 2010.
- [15] D. An, X. Tong, K. Liu, et al., "Understanding the impact of built environment on metro ridership using open source in Shanghai," Cities, vol. 93, pp. 177-187, 2019.
- [16] S. Lee and J. E. Kang, "Impact of particulate matter and urban spatial characteristics on urban vitality using spatiotemporal big data," Cities, vol. 131, p. 104030, 2022.
- [17] S. He, Z. Zhang, S. Yu, et al., "Investigating the effects of urban morphology on vitality of community life circles using machine learning and geospatial approaches," Applied Geography, vol. 167, p. 103287, 2024
- [18] M. Liu, Y. Liu, and Y. Ye, "Nonlinear effects of built environment features on metro ridership: An integrated exploration with machine learning considering spatial heterogeneity," Sustainable Cities and Society, vol. 95, p. 104613, 2023.
- [19] L. Anselin, "Local indicators of spatial association LISA," Geographical Analysis, vol. 27, no. 2, pp. 93-115, 1995.
- [20] Y. Chen, B. Yu, B. Shu, et al., "Exploring the spatiotemporal patterns and correlates of urban vitality: Temporal and spatial heterogeneity," Sustainable Cities and Society, vol. 91, p. 104440, 2023.
- [21] J. Zhao, C. Zhu, and K. Zhao, "Spatial and temporal characteristics of the impact of TOD built environment on rail transit riders' travels," IAENG International Journal of Applied Mathematics, vol. 55, no. 1, pp. 65-73, 2025.
- [22] A. Ibraeva, G. H. de Almeida Correia, C. Silva, et al., "Transit-oriented development: A review of research achievements

- and challenges," Transportation Research Part A: Policy and Practice, vol. 132, pp. 110-130, 2020.
- [23] Z. Wang, Y. Liu, X. Luo, et al., "Nonlinear relationship between urban vitality and the built environment based on multi-source data: A case study of the main urban area of Wuhan City at the weekend," Progress in Geography, vol. 42, no. 4, pp. 716-729, 2023.
 [24] P. Sulis, E. Manley, C. Zhong, et al., "Using mobility data as proxy
- [24] P. Sulis, E. Manley, C. Zhong, et al., "Using mobility data as proxy for measuring urban vitality," Journal of Spatial Information Science, no. 16, pp. 137-162, 2018.
- [25] L. Yang, B. Yu, Y. Liang, et al., "Time-varying and non-linear associations between metro ridership and the built environment," Tunnelling and Underground Space Technology, vol. 132, p. 104931, 2023.
- [26] X. Liu, X. Chen, M. Tian, et al., "Effects of buffer size on associations between the built environment and metro ridership: A machine learning-based sensitive analysis," Journal of Transport Geography, vol. 113, p. 103730, 2023.
- [27] S. He, S. Yu, P. Wei, et al., "A spatial design network analysis of street networks and the locations of leisure entertainment activities: A case study of Wuhan, China," Sustainable Cities and Society, vol. 44, pp. 880-887, 2019.
- [28] H. Zhao, J. Shi, X. Qi, et al., "Pyramid scene parsing network," in Proceedings of the IEEE Conference on Computer Vision and Pattern Recognition, 2017, pp. 2881-2890.
- [29] X. Ye and S. Rey, "A framework for exploratory space-time analysis of economic data," The Annals of Regional Science, vol. 50, no. 1, pp. 315-339, 2013.
- [30] Y. Song, J. Wang, Y. Ge, et al., "An optimal parameters-based geographical detector model enhances geographic characteristics of explanatory variables for spatial heterogeneity analysis: Cases with different types of spatial data," GIScience & Remote Sensing, vol. 57, no. 5, pp. 593-610, 2020.
- [31] B. Huang, B. Wu, and M. Barry, "Geographically and temporally weighted regression for modeling spatio-temporal variation in house prices," International Journal of Geographical Information Science, vol. 24, no. 3, pp. 383-401, 2010.

Zhiyue Ou was born in Zhongshan City, Guangdong Province, China on March 4, 2001 and received his bachelor's degree in 2023 from Xi'an Polytechnic University. He is currently a graduate student in the School of Transportation and Communications of Lanzhou Jiaotong University. His research interests include transportation big data.

Zhongning Fu was born in Chengdu, Sichuan Province, China, on November 28, 1978. She received her Ph.D. degree from the School of Traffic and Transportation at Jilin University in 2008. She is an associate professor in the School of Traffic and Transportation at Lanzhou Jiaotong University. Her research interests include logistics system planning and transportation economic analysis.